

---

# Domain Adaptation for Time Series Forecasting via Attention Sharing

---

**Xiaoyong Jin**

Department of Computer Science  
University of California Santa Barbara  
x\_jin@cs.ucsb.edu

**Youngsuk Park**

Amazon AWS AI  
pyoungsu@amazon.com

**Danielle C. Maddix**

Amazon AWS AI  
dmmaddix@amazon.com

**Yuyang Wang**

Affiliation  
Amazon AWS AI  
yuyawang@amazon.com

## Abstract

Recent years have witnessed deep neural networks gaining increasing popularity in the field of time series forecasting. A primary reason of their success is their ability to effectively capture complex temporal dynamics across multiple related time series. However, the advantages of these deep forecasters only start to emerge in the presence of a sufficient amount of data. This poses a challenge for typical forecasting problems in practice, where one either has a small number of time series, or limited observations per time series, or both. To cope with the issue of data scarcity, we propose a novel domain adaptation framework, Domain Adaptation Forecaster (DAF), that leverages the statistical strengths from another relevant domain with abundant data samples (source) to improve the performance on the domain of interest with limited data (target). In particular, we propose an attention-based shared module with a domain discriminator across domains as well as private modules for individual domains. This allows us to jointly train the source and target domains by generating domain-invariant latent features while retraining domain-specific features. Extensive experiments on various domains demonstrate that our proposed method outperforms state-of-the-art baselines on synthetic and real-world datasets.

## 1 Introduction

Similar to several other fields with predictive tasks, time series forecasting has recently benefited from the development of deep neural networks (Flunkert et al., 2017; Borovykh et al., 2017; Oreshkin et al., 2020b). While a deep forecasting model excels at capturing complex temporal dynamics from a sufficiently large time series dataset, it is often challenging in practice to collect enough data. A common solution to this data scarcity problem is to introduce another dataset with abundant data samples from a so-called *source domain* related to the dataset of interest, to which we refer as the *target domain*. For example, traffic data from an area with an abundant number of sensors (source domain) can be used to train a model to forecast the traffic flow in an area with insufficient monitoring recordings (target domain). However, deep neural networks trained on one domain can be poor at generalizing to another domain due to the issue of *domain shift*, that is, the distributional discrepancy between the source and target domains (Wang et al., 2020).

*Domain adaptation* (DA) methods attempt to mitigate the harmful effect of domain shift by aligning features extracted across source and target domains (Ganin & Lempitsky, 2015; Bousmalis et al., 2016; Hoffman et al., 2018; Bartunov & Vetrov, 2018). Existing approaches mainly focus on classification

tasks, where a classifier learns a mapping from a learned domain-invariant latent space to a fixed label space using source data. Consequently, the classifier depends only on common features across domains, and can be applied to the target domain (Wilson & Cook, 2020).

Some prior works (Zhang et al., 2019; Rennie et al., 2020) have successfully applied DA to sequence generation tasks similar to forecasting. Two main challenges still remain in directly applying existing DA methods to time series forecasting. First, the output space of a forecasting task is not shared across domains in general since a forecaster generates a time series following the input, which can be from different spaces. Second, in addition to domain-invariant features, domain-specific information needs to be extracted and incorporated in forecasting in order to guarantee that all patterns are accurately captured in predictions, and to approximate the data distribution of the target domain. Therefore, we need to carefully design the type of features to be shared or non-shared over different domains as well as to choose a suitable architecture from model classes in time-series forecasting.

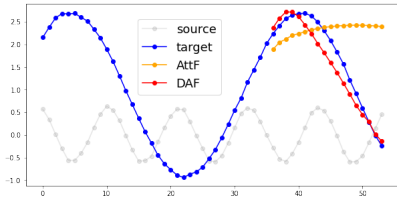


Figure 1: Accuracy comparison of attention-based forecasters (AttF) and our domain adaptation forecaster (DAF) on a data-scarce target domain provided with a data-rich source domain.

Recently, attention-based models have been effectively applied to forecasting (Li et al., 2019; Lim et al., 2019) encouraged by the success of Transformer (Vaswani et al., 2017) in natural language tasks. In addition to its superior performance under normal settings, the attention mechanism can be a suitable choice under the domain adaptation setting as well. In fact, since it consists of two steps, sequence encoding and context matching, we can make the sequence encoding utilize data from both of domains and the feature space for subsequent context matching domain-agnostic at the same time. In other words, an attention-based architecture can generate domain-aware forecasts based on encoded features from different domains by sharing the context matching module with the latent feature space it works in across domains. Figure 1

shows a motivating example, where the performance of attention-based forecasters can be significantly improved by being equipped with domain adaptation.

In this paper, we propose a novel method, the Domain Adaptation Forecaster (DAF), that effectively solves the data scarcity issue in time series forecasting by applying domain adaptation techniques to address the issue of domain shift. The main contributions of this paper are:

1. In DAF, we propose a new architecture, that properly induces, and combines domain-invariant and domain-specific features to make predictions for both source and target domains through a shared attention module. To the best of our knowledge, our model is the first attempt to apply end-to-end DA to the specific setting of time series forecasting rather than conventional pre-training and fine-tuning strategies.
2. We demonstrate that DAF outperforms other state-of-the-art baselines in terms of accuracy in a data-scarce target domain through extensive synthetic and real-world experiments that solve the cold-start and few-shot forecasting problems.
3. We perform an ablation study to show that both the choice of attention model and the domain-invariant features induced by a discriminator significantly improves the accuracy of DAF.

The outline of the paper is as follows. We provide an overview of related works and their limitations in section 2. In section 3, we formally define the time series forecasting problem, and review preliminaries about the domain adaptation and basic attention models. We present our model, the Domain Adaptation Forecaster (DAF) in section 4, and demonstrate its effectiveness in section 5, followed by concluding remarks in section 6.

## 2 Related Work

Deep learning based time series forecasting models usually consist of a sequential feature encoder that extracts key information from an observed history using various architectures (Flunkert et al., 2017; Borovykh et al., 2017; Oreshkin et al., 2020b), and a decoder that generates predictions based on learned representations with global-local hierarchy (Wen et al., 2017; Wang et al., 2019) or specific function space bases (Fox et al., 2018; Rangapuram et al., 2018). Recently, attention-based transformer-like models (Vaswani et al., 2017) have also been introduced to the forecasting community and achieved state-of-the-art performance (Li et al., 2019; Lim et al., 2019; Wu et al.,

2020; Zhou et al., 2021). A downside to these sophisticated models is that they require a large dataset with homogeneous time series to train. Once trained, the deep learning models do not generalize well to a new domain of exogenous data due to domain shift issues.

To solve the domain shift issue, domain adaptation has been proposed to transfer knowledge captured from a source domain with sufficient data to the target domain with unlabeled or insufficiently labeled data for both vision and language tasks (Motiian et al., 2017; Wilson & Cook, 2020; Ramponi & Plank, 2020). In particular, sequence modeling tasks in natural language processing mainly adopt a paradigm where large transformers are successively pre-trained on a general domain and fine-tuned on the task domain (Devlin et al., 2018; Han & Eisenstein, 2019; Gururangan et al., 2020; Rietzler et al., 2020). In spite of the success in NLP, it is not immediate to directly apply those methods to forecasting scenarios due to several essential differences. First, it is hard to find a common source dataset in time series forecasting to pre-train a large forecasting model unlike in NLP, and it is expensive to pre-train a different model for each target domain. Second, the predicted values are not subject to a fixed vocabulary, heavily relying on extrapolation. Moreover, there are many domain-specific confounding factors that cannot be encoded by a pre-trained model. For example, Oreshkin et al. (2020a) aims to learn a meta forecasters that makes zero-shot forecasts, but it can only support univariate time series forecasting.

A dominant approach for domain adaptation is to learn domain-invariant representations of raw data (Ben-David et al., 2010; Cortes & Mohri, 2011; Ganin & Lempitsky, 2015). These models typically employ a feature extractor that maps raw data from each domain into a domain-invariant latent space, and a recognition model that learns a correspondence between these representations and the labels using source data (Tzeng et al., 2017; Zhang et al., 2017; Chen et al., 2019b). Various approaches have been explored to align the representations from both target and source domains. While the work like Long et al. (2015); Chen et al. (2019a); Guo et al. (2020) aims to minimize a well-defined discrepancy measure between latent distributions between domains, adversarial training that employs a domain discriminator to distinguish representations from different domains has been more popular in sequence labeling tasks recently due to its superior performance (Tzeng et al., 2017; Zhao et al., 2018; Alam et al., 2018; Du et al., 2020; Wright & Augenstein, 2020). In light of these successes, Hu et al. (2020) attempts to adopt adversarial training in fine-tuning the pre-trained forecasting model by augmenting target dataset with source data selected based on defined metrics. However, traditional adversarial training methods focus only on domain-invariant features, yet domain-specific features are also necessary to make domain-related predictions in a regression task as forecasting. In this regard, a series of work (Ghifary et al., 2016; Bousmalis et al., 2016; Shi et al., 2018) make use of both the domain-invariant and domain-specific representations by reconstructing the input from different domains in the meantime of adaptation. Nevertheless, these methods do not account for the sequential nature of time series and cannot be directly applied to forecasting.

### 3 Domain Adaptation in Forecasting

**Time Series Forecasting** Suppose we have a set of  $N$  time series, each of which consists of observations  $z_{i,t} \in \mathbb{R}$  with optional input covariates  $\xi_{i,t} \in \mathbb{R}^d$  at time  $t$ . Example input covariates include price and promotion at a certain time. In time series forecasting, given  $T$  past observations and all future input covariates, we wish to make  $\tau$  future predictions at time  $T$ :

$$z_{i,T+1}, \dots, z_{i,T+\tau} = F(z_{i,1}, \dots, z_{i,T}, \xi_{i,1}, \dots, \xi_{i,T+\tau}), \quad (1)$$

where  $F$  is a deterministic or probabilistic model. In this paper, we focus on the scenario where there is little data available for the problem of interest while another time series dataset with sufficient amount of information is available. The lack of data occurs when the number of time series  $N$  is small, or the length  $T$  is limited, or both.

For notation simplicity, we drop the covariates  $\{\xi_{i,t}\}_{t=1}^{T+\tau}$  from the following definitions. We denote the dataset  $\mathcal{D} = \{(\mathbf{X}_i, \mathbf{Y}_i)\}_{i=1}^N$  with past observations  $\mathbf{X}_i = [z_{i,t}]_{t=1}^T$  and future ground truths  $\mathbf{Y}_i = [z_{i,t}]_{t=T+1}^{T+\tau}$  for the  $i$ -th time series. We omit the index  $i$  when the context is clear.

**Adversarial Domain Adaptation in Forecasting** To find a good forecasting model  $F$  in equation (1) on a data-scarce time series dataset, we cast the problem in terms of a domain adaptation problem, given that another “relevant” dataset is accessible. In the domain adaption setting, we have two types of data: source data  $\mathcal{D}_S$  with abundant samples and target data  $\mathcal{D}_T$  with limited samples. Our goal is to produce an accurate forecast on the target domain  $\mathcal{T}$ , where little data is available,

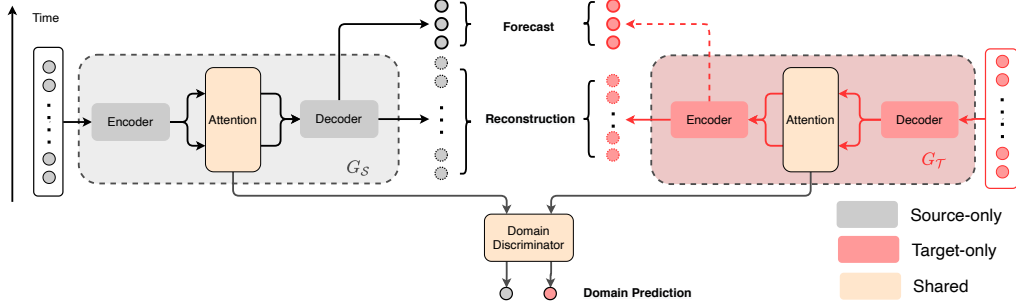


Figure 2: An architectural overview of DAF. The grey modules belong to the source domain, and red modules belong to target domain. The attention modules and domain discriminators shown in beige are shared by both domains. The model takes the historical portion of a time series as input, and produces a reconstruction of input and a forecast of the future time steps. The domain discriminator is a binary classifier, and predicts the origin of an intermediate representation within the attention module, either the source or the target.

by leveraging the data in the source domain  $\mathcal{S}$ . Since our goal is to provide a forecast in the target domain, in the remainder of the text, we use  $T$  and  $\tau$  to denote the target historical length and target prediction length, respectively, and also use the subscript  $\mathcal{S}$  for the corresponding quantities in the source data  $\mathcal{D}_\mathcal{S}$ , and likewise for  $\mathcal{T}$ .

To compute the desired target prediction  $\hat{\mathbf{Y}}_i = [\hat{z}_{i,t}]_{t=T+1}^{T+\tau}$ ,  $i = 1, \dots, N$ , we optimize the training error on both domains jointly and in an adversarial manner in the following minimax problem:

$$\min_{G_\mathcal{S}, G_\mathcal{T}} \max_D \mathcal{L}_{seq}(\mathcal{D}_\mathcal{S}; G_\mathcal{S}) + \mathcal{L}_{seq}(\mathcal{D}_\mathcal{T}; G_\mathcal{T}) - \lambda \mathcal{L}_{dom}(\mathcal{D}_\mathcal{S}, \mathcal{D}_\mathcal{T}; D, G_\mathcal{S}, G_\mathcal{T}), \quad (2)$$

where the parameter  $\lambda \geq 0$  balances between the estimation error  $\mathcal{L}_{seq}$  and the domain classification error  $\mathcal{L}_{dom}$ . Here,  $G_\mathcal{S}, G_\mathcal{T}$  denote sequence generators that estimate sequences in each domain, respectively, and  $D$  denotes a discriminator that classifies the domain between source and target.

We first define the estimation error  $\mathcal{L}_{seq}$  induced by a sequence generator  $G$  as follows:

$$\mathcal{L}_{seq}(\mathcal{D}; G) = \sum_{i=1}^N \left( \underbrace{\frac{1}{T} \sum_{t=1}^T l(z_{i,t}, \hat{z}_{i,t})}_{\text{reconstruction error}} + \underbrace{\frac{1}{\tau} \sum_{t=T+1}^{T+\tau} l(z_{i,t}, \hat{z}_{i,t})}_{\text{prediction error}} \right), \quad (3)$$

where  $l$  is a loss function and estimation  $\hat{z}_{i,t}$  is the output of a generator  $G$ , and each term in equation (3) represents the error of input reconstruction and future prediction, respectively. Next, let  $\mathcal{H} = \{H_i\}_{i=1}^N$  be the set of some latent feature  $h_{i,t}$  induced by generator  $G$ . Then, the domain classification error  $\mathcal{L}_{dom}$  in equation (2) is the cross-entropy loss in latent spaces as follows:

$$\mathcal{L}_{dom}(\mathcal{D}_\mathcal{S}, \mathcal{D}_\mathcal{T}; D, G_\mathcal{S}, G_\mathcal{T}) = -\frac{1}{|\mathcal{H}_\mathcal{S}|} \sum_{h_{i,t} \in \mathcal{H}_\mathcal{S}} \log D(h_{i,t}) - \frac{1}{|\mathcal{H}_\mathcal{T}|} \sum_{h_{i,t} \in \mathcal{H}_\mathcal{T}} \log [1 - D(h_{i,t})], \quad (4)$$

where  $\mathcal{H}_\mathcal{S}$  and  $\mathcal{H}_\mathcal{T}$  are latent feature sets associated with the source  $\mathcal{D}_\mathcal{S}$  and target  $\mathcal{D}_\mathcal{T}$ , and  $|\mathcal{H}|$  denotes the cardinality of a set  $\mathcal{H}$ . In the end, objective equation (2) is maximized with respect to  $D$  and minimized with respect to  $G_\mathcal{S}, G_\mathcal{T}$  via adversarial training. In section 4, we propose specific design choices for  $G_\mathcal{S}, G_\mathcal{T}$  and the latent features  $\mathcal{H}_\mathcal{S}, \mathcal{H}_\mathcal{T}$  in our DAF model.

#### 4 Our Methodology: The Domain Adaptation Forecaster (DAF)

Conventional DA methods explicitly align the representations of the entire input sequence for knowledge transfer between domains. In time series forecasting problems with dynamical patterns, local representations within a time period are likely to be more important for future predictions than others. Since attention mechanisms explicitly search for relevant historical patterns by context matching, we propose the strategy of attention sharing to perform domain adaptation in forecasting. Figure 2 provides an overview of the proposed architecture. Specifically, the pairwise alignment metrics of local patterns along time computed by equation (5) are independent of specific patterns,

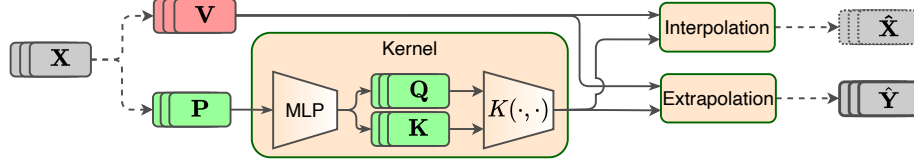


Figure 3: In DAF, the shared attention module processes pattern and value embeddings from either domain. A kernel function encodes pattern embeddings to a shared latent space for weight computation. We combine value embeddings by different groups of weights to obtain the interpolation  $t \leq T$  for reconstruction  $\hat{\mathbf{X}}$  and the extrapolation  $t = T + 1$  for the prediction output  $\hat{\mathbf{Y}}$ .

and are universally applicable to either domain. Since the queries and keys are only involved in the domain-agnostic attention, and the values constitute the predictions, it is feasible to explicitly align the queries and keys while keeping the values domain-specific for adaptation. In our proposed DAF model, we employ encoders that are privately owned by each domain to extract patterns and values. We use a shared attention module to compute similarity scores by domain-invariant queries and keys. Lastly, private decoders map the attention outputs into data spaces of each domain accordingly.

#### 4.1 Sequence Generator

In this subsection, we discuss our design of the sequence generators  $G_S, G_T$  in equation (2). Since the generators for both domains have the same architecture, we omit the domain index of all quantities and denote either generator by  $G$  in the following subsections by default. The generator  $G$  in each domain processes an input time series  $\mathbf{X} = [z_t]_{t=1}^T$  in the following order: private encoders, shared attention, and private decoder, to generate the reconstructed sequence  $\hat{\mathbf{X}}$  and the predicted future  $\hat{\mathbf{Y}}$ . Note that instead of a sequence-to-sequence models, e.g. a vanilla transformer where encoder and decoder possess a separate attention module,  $G$  is a sequential model with one attention module.

**Private Encoders** The private encoder transforms the raw input  $\mathbf{X}$  into the pattern embedding  $\mathbf{P} = [\mathbf{p}_t]_{t=1}^T$  and value embedding  $\mathbf{V} = [\mathbf{v}_t]_{t=1}^T$ . For the pattern embedding  $\mathbf{P}$ , we apply  $M$  separate convolutions with various kernel sizes in order to extract multi-scale local patterns. For  $j = 1, \dots, M$ , each convolution takes a sequence  $\mathbf{X}$  to give sequence  $\mathbf{P}^j = [\mathbf{p}_t^j]_{t=1}^T$

$$\mathbf{P}^j = \text{Conv}(\mathbf{X}; \theta_p^j),$$

where  $\theta_p^j$  is the weight parameters. We concatenate each  $\mathbf{p}_t^j$  to build a multi-scale pattern  $\mathbf{p}_t = [\mathbf{p}_t^j]_{j=1}^M$  and  $\mathbf{P} = [\mathbf{p}_t]_{t=1}^T$  with parameters  $\theta_p = [\theta_p^j]_{j=1}^M$  accordingly. For the value embedding  $\mathbf{V} = [\mathbf{v}_t]_{t=1}^T$ , we apply a position-wise MLP to  $\mathbf{X} = [z_t]_{t=1}^T$ :

$$\mathbf{v}_t = \text{MLP}(z_t; \theta_v).$$

The extracted pattern  $\mathbf{P}$  and value  $\mathbf{V}$  are fed into the shared attention module.

**Shared Attention Module** As shown in Figure 7, the shared attention module aims to build the queries and the keys from the embeddings  $\mathbf{P}$  and  $\mathbf{V}$  from both source and target domain. Formally, we project pattern embeddings  $\mathbf{P}$  into  $d$ -dimensional queries  $\mathbf{Q} = [\mathbf{q}_t]_{t=1}^T$  and keys  $\mathbf{K} = [\mathbf{k}_t]_{t=1}^T$  via a position-wise MLP:

$$(\mathbf{q}_t, \mathbf{k}_t) = \text{MLP}(\mathbf{p}_t; \theta_s).$$

Intuitively, the patterns from both domains are projected into a common space, which is then induced to be domain-invariant (see section 4.2), for comparison in the subsequent attention operation. Specifically, at time  $t$ , an attention score  $\alpha$  is computed as the alignment score between the query  $\mathbf{q}_t$  and keys  $\mathbf{k}_{t'}$  at neighborhood positions  $t' \in \mathcal{N}(t)$  using a positive semi-definite kernel  $\mathcal{K}(\cdot, \cdot)$ ,

$$\alpha(\mathbf{q}_t, \mathbf{k}_{t'}) = \frac{\mathcal{K}(\mathbf{q}_t, \mathbf{k}_{t'})}{\sum_{t' \in \mathcal{N}(t)} \mathcal{K}(\mathbf{q}_t, \mathbf{k}_{t'})}. \quad (5)$$

e.g. an exponential scaled dot-product  $\mathcal{K}(\mathbf{q}, \mathbf{k}) = \exp\left(\frac{\mathbf{q}^T \mathbf{k}}{\sqrt{d}}\right)$ . Then, the representation  $\mathbf{o}_t$  is averaged over values  $\mathbf{v}_{\mu(t')}$  weighted by attention score  $\alpha(\mathbf{q}_t, \mathbf{k}_{t'})$  on neighborhood  $\mathcal{N}(t)$ , followed

---

**Algorithm 1** Adversarial Training of DAF

---

```
1: Input: dataset  $\mathcal{D}_S, \mathcal{D}_T$ ; epochs  $E$ , step sizes  
2: Initialization: parameter  $\Theta_G$  for generator  $G_S, G_T$ , parameter  $\theta_D$  for discriminator  $D$   
3: for epoch = 1 to  $E$  do  
4:   repeat  
5:     sample  $\mathbf{X}_S, \mathbf{Y}_S \sim \mathcal{D}_S$  and  $\mathbf{X}_T, \mathbf{Y}_T \sim \mathcal{D}_T$   
6:     generate  $\hat{\mathbf{X}}_S, \hat{\mathbf{Y}}_S = G_S(\mathbf{X}_S)$  and  $\hat{\mathbf{X}}_T, \hat{\mathbf{Y}}_T = G_T(\mathbf{X}_T)$   
7:     compute  $\mathcal{L}_{seq}$  in equation (3) for  $S$  and  $T$ ,  $\mathcal{L}_{dom}$  in equation (4), and total  $\mathcal{L}$  in equation (2)  
8:     gradient descent with  $\nabla_{\Theta_G} \mathcal{L}$  to update  $G_S, G_T$   
9:     gradient ascent with  $\nabla_{\theta_D} \mathcal{L}$  to update  $D$   
10:   until  $\mathcal{D}_T$  is exhausted  
11: end for
```

---

by a MLP with parameter  $\theta_o$ :

$$\mathbf{o}_t = \text{MLP} \left( \sum_{t' \in \mathcal{N}(t)} \alpha(\mathbf{q}_t, \mathbf{k}_{t'}) \mathbf{v}_{\mu(t')}; \theta_o \right),$$

where  $\mu : \mathbb{N} \rightarrow \mathbb{N}$  is a position translation. The choice of  $\mathcal{N}(t)$  and  $\mu(t)$  depends on whether  $G$  is in interpolation mode for reconstruction when  $t \leq T$  or extrapolation mode for forecasting when  $t > T$ . See section A for details on interpolation and extrapolation with  $\mathcal{N}(t)$  and  $\mu(t)$  selection.

**Private Decoders** The private decoder in each domain produces output  $\hat{z}_t$  from  $\mathbf{o}_t$  through another position-wise MLP:  $\hat{z}_t = \text{MLP}(\mathbf{o}_t; \theta_d)$ . By doing so, we can generate reconstructions  $\hat{\mathbf{X}} = [\hat{z}_t]_{t=1}^T$  as well as the one-step prediction  $\hat{z}_{T+1}$ . This prediction  $\hat{z}_{T+1}$  is fed as input into the private encoder and attention model to predict the next one-step ahead prediction. Finally, we feed the prior predictions recursively to generate the entire prediction  $\hat{\mathbf{Y}} = [\hat{z}_t]_{t=T+1}^{T+\tau}$  over  $\tau$  time steps.

## 4.2 Domain Discriminator

We would like to induce the queries and keys of the shared attention module to be domain-invariant, so that the process of context matching in equation (5) can ideally be universal across domains. To encourage these features to be aligned in the same latent space, we introduce a domain discriminator  $D : \mathbb{R}^d \rightarrow [0, 1]$  as a position-wise MLP:

$$D(\mathbf{q}_t) = \text{MLP}(\mathbf{q}_t; \theta_D), \quad D(\mathbf{k}_t) = \text{MLP}(\mathbf{k}_t; \theta_D).$$

The discriminator  $D$  performs binary classifications on whether  $\mathbf{q}_t$  and  $\mathbf{k}_t$  originate from the source or target domain by minimizing cross entropy loss of  $\mathcal{L}_{dom}$  in equation (4). We design the latent features  $\mathcal{H}_S, \mathcal{H}_T$  in equation (4) to be the keys  $\mathbf{K} = [\mathbf{k}_t]_{t=1}^T$  and queries  $\mathbf{Q} = [\mathbf{q}_t]_{t=1}^T$  in both source and target domains, respectively.

## 4.3 Adversarial Training

Recall we have defined generators  $G_S, G_T$  based on the private encoder/decoder and the shared attention module. The discriminator  $D$  induces the invariance of latent features keys  $\mathbf{K}$  and queries  $\mathbf{Q}$  across domains. While  $D$  tries to classify the domain between source and target,  $G_S, G_T$  are trained to confuse  $D$ . By choosing the MSE loss for  $l$ , the minimax objective in equation (2) is now formally defined over generators  $G_S, G_T$  with parameters  $\Theta_G = \{\theta_p^S, \theta_v^S, \theta_d^S, \theta_p^T, \theta_v^T, \theta_d^T, \theta_s, \theta_o\}$  and domain discriminator  $D$  with parameter  $\theta_D$ . Algorithm 1 summarizes the training routine of DAF. We alternately update  $\Theta_G$  and  $\theta_D$  in opposite directions so that  $G = \{G_S, G_T\}$  and  $D$  are trained adversarially. Here, we use a standard pre-processing for  $\mathbf{X}, \mathbf{Y}$  and post-processing for  $\hat{\mathbf{X}}, \hat{\mathbf{Y}}$ .

## 5 Experiments

We perform empirical studies on synthetic and real-world benchmark datasets. Our extensive experiments demonstrate the effectiveness of transferring knowledge from a data rich source domain



Task	$N$	$T$	$\tau$	DAR	VT	CT	AttF	MetaF	PTF	RDA	DAF
Cold Start	5000	36	18	0.053	0.040	0.042	0.042	0.045	0.039	<b>0.035</b>	<b>0.035</b>
		45		0.037	0.039	0.041	0.037	0.043	0.037	0.034	<b>0.030</b>
		54		<b>0.031</b>	0.039	0.038	0.037	0.042	0.034	0.034	<b>0.029</b>
Few Shot	20	144		0.062	0.089	0.095	0.074	0.071	0.086	<b>0.059</b>	<b>0.057</b>
	50			0.059	0.085	0.074	0.063	0.061	0.086	<b>0.054</b>	<b>0.055</b>
	100			0.059	0.079	0.071	0.059	0.053	0.081	0.053	<b>0.051</b>

Table 1: Performance comparison of DAF on synthetic datasets with varying historical lengths  $T$  (cold-start), and varying number of time series  $N$  (few-shot) and prediction length  $\tau$  in terms of the mean ND metric. The winners and the competitive followers (the gap is smaller than its standard deviation over 5 runs) are bolded for reference.

to a data scarce target domain via the proposed DAF, leading to accuracy improvement over several deep learning and DA state-of-the-art models on these problems. In addition, we conduct an ablation study to provide understanding on how much each component of DAF contribute to the improvement.

### 5.1 Baselines and Evaluation

Throughout experiments and ablation studies, we compare DAF with the following baselines. Conventional single-domain forecasters trained only on the target domain:

- DAR: RNN-based DeepAR (Flunkert et al., 2017);
- VT: Vanilla Transformer (Vaswani et al., 2017);
- CT: Attention-based ConvTrans (Li et al., 2019);
- AttF: Attention Forecaster without attention module sharing and domain adaptation, equivalent to DAF without referring to source data. AttF is similar to CT but has a different objective function.

Cross-domain forecasters trained on both source and target domain:

- MetaF: Zero-shot meta-forecaster (Oreshkin et al., 2020a);
- PTF: Pretrained forecaster based on the sequence generator of DAF, i.e. a sequence generator is trained using source data, and finetuned with target data;
- RDA: RNN-based DA forecaster obtained by replacing the attention module in DAF with an LSTM module and inducing the domain-invariance of LSTM encodings;
- NA-DAF: Non-adversarial DAF without the domain discriminator  $D$ .

We implement the models using PyTorch (Paszke et al., 2019), and train them on AWS Sagemaker (Liberty et al., 2020). For DAR, we call the publicly available version on Sagemaker. In most of the experiments, DAF and the baselines are tuned on a held-out validation set. For details on the model configurations and hyperparameter selections, see section C.2.

We evaluate the forecasting error in terms of the Normalized Deviation (ND) (Yu et al., 2016): 
$$ND = \left( \sum_{i=1}^N \sum_{t=T+1}^{T+\tau} |z_{i,t} - \hat{z}_{i,t}| \right) / \left( \sum_{i=1}^N \sum_{t=T+1}^{T+\tau} |z_{i,t}| \right)$$
 where  $\mathbf{Y}_i = [z_{i,t}]_{t=T+1}^{T+\tau}$  and  $\hat{\mathbf{Y}}_i = [\hat{z}_{i,t}]_{t=T+1}^{T+\tau}$  are the ground truths and predictions, respectively. In the subsequent tables, the methods with a mean ND metric within one standard deviation of method with the lowest mean ND metric are shown in bold. See Table 6 and Table 7 in supplemental materials for the results including the mean and standard deviations computed over 5 runs.

### 5.2 Synthetic Datasets

We conduct a synthetic study to simulate scenarios suited for domain adaptation, namely **cold-start** and **few-shot** forecasting. The total observations are limited in both scenarios by either length or number of time series, and the effectiveness of DAF in each scenario is observed individually. In both scenarios, we consider a source dataset  $\mathcal{D}_S$  and a target dataset  $\mathcal{D}_T$  consisting of time-indexed sinusoidal signals with random parameters, including amplitude, frequency and phases, sampled from different uniform distributions. See section B for details on the data generation.

**Cold-start** forecasting aims to forecast in a target domain, where the signals are fairly short and limited historical information is available for future predictions. To simulate solving the cold-start problem, we set the time series historical length in the source data  $T_S = 144$ , and vary the historical

$\mathcal{D}_T$	$\mathcal{D}_S$	$F$	$T$	$\tau$	DAR	VT	CT	MetaF	PTF	RDA	DAF
<i>traf</i>	<i>elec</i>	H	168	24	0.205	0.187	0.183	0.190	0.184	0.174	<b>0.169</b>
	<i>wiki</i>							0.188	0.185	0.181	<b>0.176</b>
<i>elec</i>	<i>traf</i>				0.141	0.144	0.131	0.151	0.144	0.154	<b>0.125</b>
	<i>sales</i>							0.144	0.138	0.142	<b>0.123</b>
<i>wiki</i>	<i>sales</i>	D	28	7	0.055	0.061	0.051	0.061	<b>0.047</b>	<b>0.049</b>	<b>0.049</b>
	<i>traf</i>							0.059	<b>0.044</b>	<b>0.045</b>	<b>0.042</b>
<i>sales</i>	<i>wiki</i>				0.305	0.293	0.324	0.311	0.292	<b>0.287</b>	<b>0.280</b>
	<i>elec</i>							0.329	0.287	0.285	<b>0.277</b>

Table 2: Performance comparison of DAF on real-world benchmark datasets with the historical time series length  $T$ , prediction length  $\tau$ , in the target domain determined by the target dataset frequencies  $F$  in terms of the mean ND metric. The winners and the competitive followers (the gap is smaller than its standard deviation over 5 runs) are bolded for reference.

length in the target data  $T$  within  $\{36, 45, 54\}$ . The period of sinusoids in the target domain is fixed to be 36, so that the historical observations cover  $1 \sim 1.5$  periods. We also fix the number of time series  $N_S = N = 5000$ .

**Few-shot** forecasting occurs when there are an insufficient number of time series in the target domain for a well-trained forecaster. To simulate this problem, we set the number of time series in the source data  $N_S = 5000$ , and vary the number of time series in the target data  $N$  within  $\{20, 50, 100\}$ . We also fix the historical lengths  $T_S = T = 144$ .

The prediction length is set to be equal for both source and target datasets, i.e.  $\tau_S = \tau = 18$ . The results of the synthetic experiments on the cold-start and few-shot problems in Table 1 demonstrate that the performance of DAF is better than or on par with the baselines in all experiments. We also note the following four observations to provide a better understanding into domain adaptation methods. First, we see that the cross-domain forecasters except for PTF are overall more accurate than the single-domain forecasters. This finding indicates that source data is helpful in forecasting the target data. Second, among the cross-domain forecasters, PTF is less accurate than RDA and DAF, and even less than the single-domain forecaster DAR. This result shows the limitations of the pretrain-finetune strategy compared to DA methods. Third, on a majority of the experiments our attention-based DAF model is more accurate than or competitive to the RNN-based DA (RDA) method. Moreover, we observe that DAF improves more significantly as the number of training samples becomes smaller in Figure 4. A more thorough demonstration can be found in section D.

### 5.3 Real-World Datasets

We perform experiments on four real benchmark datasets that are widely used in forecasting literature: *elec* and *traf* from the UCI data repository (Dua & Graff, 2017), and *sales* (kaggle, a), *wiki* (kaggle, b) from kaggle. The *elec* and *traf* datasets present clear daily and weekly patterns while *sales* and *wiki* are less regular and more challenging to forecast overall. We use the following time features  $\xi_t \in \mathbb{R}^2$  as covariates: the day of the week and hour of the day for the hourly datasets *elec* and *traf*, and the day of the month and day of the week for the daily datasets *sales* and *wiki*. For more dataset details, see section B.

To evaluate the performance of DAF, we consider cross-dataset adaptation, i.e., transferring between a pair of datasets. Since the original datasets are large enough to train a reasonably good forecaster, we only take a subset of each dataset as a target domain to simulate the data-scarce situation. Specifically, we take the last 30 days of each time series in the hourly dataset *elec* and *traf*, and the last 60 days from daily dataset *sales* and *wiki*. We partition the target datasets equally into training/validation/test splits, i.e. 10/10/10 days for hourly datasets and 20/20/20 days for daily datasets. The full datasets are used as source domains in adaptation. We follow the rolling window strategy from Flunkert et al. (2017), and split each window into historical and prediction time series of lengths  $T$  and  $T + \tau$ , respectively. In our experiments, we set  $T = 168, \tau = 24$  for hourly datasets, and  $T = 28, \tau = 7$  for the daily datasets. For DA methods, the splitting of the source data follows analogously.

Table 2 shows that the conclusions drawn from Table 1 on the synthetic experiments generally hold on the real-world datasets. In particular, we see the accuracy improvement by DAF over the baselines is more significant than that in the synthetic experiments. The real-world experiments also demonstrate that in general the success of DAF is agnostic of the source domain, and is even effective



when transferring from a source domain of different frequency than that of the target domain. In addition, the cross-domain forecasters, PTF, RDA and our DAF outperform the three single-domain baselines in most cases, whereas the cross-domain forecaster MetaF has similar performance as its single-domain counterpart N-BEATS. Unlike PTF, our DAF method has consistent and accurate performance on both synthetic and real-world experiments. The accuracy differences between DAF and RDA are larger than in the synthetic case, and in favor of DAF. This finding further demonstrates that our choice of an attention-based architecture is well-suited for real domain adaptation problems.

Remarkably, DAF manages to learn the different patterns between source and target domain. For instance, Figure 5 illustrates that DAF can successfully learn clear daily patterns in the *traf* dataset, and still find irregular patterns in the *sales* dataset. We argue that the reason of the success is that the private encoders with multi-scale structures are able to extract frequency-agnostic features while the attention module is able to reconstruct frequency information by pattern matching in the common latent space of queries and keys, and the domain-specific decoders are able to make distinct forecasts.

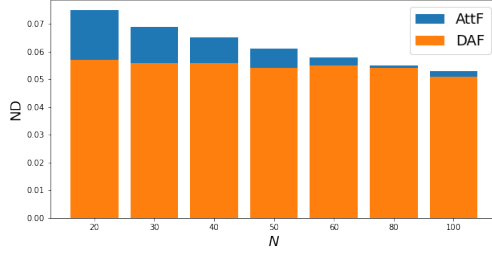


Figure 4: Forecasting accuracy of AttF and DAF methods in synthetic few-shot experiments with different target dataset sizes.

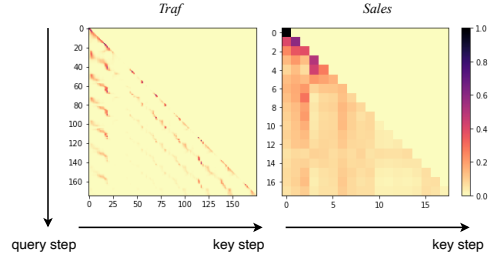


Figure 5: Attention distribution produced by one of the attention heads of DAF with  $\mathcal{D}_S = \text{traf}$  (left) and  $\mathcal{D}_T = \text{sales}$  (right).

$\mathcal{D}_T$	$\mathcal{D}_S$	$\tau$	AttF	NA-DAF	DAF
<i>traf</i>	<i>elec</i>	24	0.194	0.172	<b>0.168</b>
<i>elec</i>	<i>traf</i>	24	0.141	0.121	<b>0.119</b>
<i>wiki</i>	<i>sales</i>	7	0.045	0.042	<b>0.041</b>
<i>sales</i>	<i>wiki</i>	7	0.314	0.294	<b>0.280</b>

Table 3: Results of ablation study in four adaptation tasks on real-world datasets

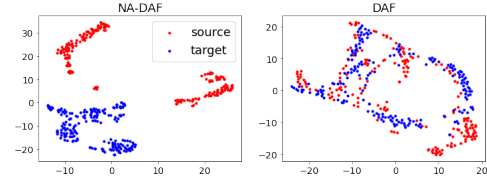


Figure 6: Query alignment with (DAF: right) and without adversarial training (NA-DAF: left), where  $\mathcal{D}_S = \text{elec}$  and  $\mathcal{D}_T = \text{traf}$ .

## 5.4 Ablation Study

Our proposed DAF model relies on two components: the shared attention module and the adversarial discriminator, to transfer between domains. In order to examine each of their contributions to domain adaptation, we conduct an ablation study by removing the two components successively. Specifically, we consider two variants of DAF defined in section 5.1: the single-domain attention-based forecaster AttF and the cross-domain forecaster without the adversarial domain discriminator NA-DAF.

The results in Table 3 compare the performances of DAF and its variants on the target domain in four adaptation tasks. We see that DAF and NA-DAF are more accurate than the non-DA model AttF, indicating that attention module sharing is able to transfer knowledge learned in a source domain to guide forecasting in target domain. Equipped with the domain discriminator, DAF further improves its effectiveness of adaptation compared to NA-DAF.

Intuitively, DAF benefits from an aligned latent space of queries and keys across domains. Figure 6 visualizes the distribution of queries and keys learned in the forecasting task, where the target data  $\mathcal{D}_T = \text{traf}$  and the source data  $\mathcal{D}_S = \text{elec}$  via a TSNE embedding. Empirically, we see the latent distributions are well aligned in DAF but not in NA-DAF, which can explain the improved performance of DAF over its variants.

## 6 Conclusion

In this paper, we aim to apply domain adaptation to time series forecasting to solve the data scarcity problem. We identify the differences between forecasting task and common domain adaptation scenarios, and accordingly propose the Domain Adaptation Forecaster (DAF) based on attention sharing. Through empirical experiments, we demonstrate that our proposed model is able to effectively transfer knowledge from a data-rich domain for accurate forecasts in a data-scarce domain, and outperform state-of-the-art forecasters without domain adaptation and transfer learning on synthetic and real-world datasets. Like in other areas, the theoretical justification of having domain-invariant features or properties of attention models remains an open problem. In addition, more architectural options with more sophisticated hyperparameter selections are worth exploring in the future work.

## References

- Alam, F., Joty, S., and Imran, M. Domain Adaptation with Adversarial Training and Graph Embeddings. In *Proceedings of the 56th Annual Meeting of the Association for Computational Linguistics (Volume 1: Long Papers)*, pp. 1077–1087, Melbourne, Australia, 2018. Association for Computational Linguistics. doi: 10.18653/v1/P18-1099. URL <http://aclweb.org/anthology/P18-1099>.
- Bartunov, S. and Vetrov, D. P. Few-shot Generative Modelling with Generative Matching Networks. *International Conference on Artificial Intelligence and Statistics*, pp. 670–678, 2018.
- Ben-David, S., Blitzer, J., Crammer, K., Kulesza, A., Pereira, F., and Vaughan, J. W. A theory of learning from different domains. *Machine Learning*, 79(1-2):151–175, May 2010. ISSN 0885-6125, 1573-0565. doi: 10.1007/s10994-009-5152-4. URL <http://link.springer.com/10.1007/s10994-009-5152-4>.
- Borovykh, A., Bohte, S., and Oosterlee, C. W. Conditional time series forecasting with convolutional neural networks. *arXiv preprint arXiv:1703.04691*, 2017.
- Bousmalis, K., Trigeorgis, G., Silberman, N., Krishnan, D., and Erhan, D. Domain Separation Networks. *arXiv:1608.06019 [cs]*, August 2016. URL <http://arxiv.org/abs/1608.06019>. arXiv: 1608.06019.
- Chen, C., Fu, Z., Chen, Z., Jin, S., Cheng, Z., Jin, X., and Hua, X.-S. HoMM: Higher-order Moment Matching for Unsupervised Domain Adaptation. *arXiv:1912.11976 [cs]*, December 2019a. URL <http://arxiv.org/abs/1912.11976>. arXiv: 1912.11976.
- Chen, M.-H., Kira, Z., AlRegib, G., Yoo, J., Chen, R., and Zheng, J. Temporal Attentive Alignment for Large-Scale Video Domain Adaptation. *Proceedings of the IEEE International Conference on Computer Vision*, pp. 6321–6330, 2019b.
- Cortes, C. and Mohri, M. Domain Adaptation in Regression. In Kivinen, J., Szepesvári, C., Ukkonen, E., and Zeugmann, T. (eds.), *Algorithmic Learning Theory*, volume 6925, pp. 308–323. Springer Berlin Heidelberg, Berlin, Heidelberg, 2011. ISBN 978-3-642-24411-7 978-3-642-24412-4. doi: 10.1007/978-3-642-24412-4\_25. URL [http://link.springer.com/10.1007/978-3-642-24412-4\\_25](http://link.springer.com/10.1007/978-3-642-24412-4_25). Series Title: Lecture Notes in Computer Science.
- Devlin, J., Chang, M.-W., Lee, K., and Toutanova, K. BERT: Pre-training of Deep Bidirectional Transformers for Language Understanding. *arXiv:1810.04805 [cs]*, October 2018. URL <http://arxiv.org/abs/1810.04805>. arXiv: 1810.04805.
- Du, C., Sun, H., Wang, J., Qi, Q., and Liao, J. Adversarial and Domain-Aware BERT for Cross-Domain Sentiment Analysis. In *Proceedings of the 58th Annual Meeting of the Association for Computational Linguistics*, pp. 4019–4028, Online, 2020. Association for Computational Linguistics. doi: 10.18653/v1/2020.acl-main.370. URL <https://www.aclweb.org/anthology/2020.acl-main.370>.
- Dua, D. and Graff, C. *UCI Machine Learning Repository*. University of California, Irvine, School of Information and Computer Sciences, 2017. URL <http://archive.ics.uci.edu/ml>.

- Flunkert, V., Salinas, D., and Gasthaus, J. DeepAR: Probabilistic Forecasting with Autoregressive Recurrent Networks. *arXiv:1704.04110 [cs, stat]*, April 2017. URL <http://arxiv.org/abs/1704.04110>. arXiv: 1704.04110.
- Fox, I., Ang, L., Jaiswal, M., Pop-Busui, R., and Wiens, J. Deep Multi-Output Forecasting: Learning to Accurately Predict Blood Glucose Trajectories. In *Proceedings of the 24th ACM SIGKDD International Conference on Knowledge Discovery & Data Mining - KDD '18*, pp. 1387–1395, London, United Kingdom, 2018. ACM Press. ISBN 978-1-4503-5552-0. doi: 10.1145/3219819.3220102. URL <http://dl.acm.org/citation.cfm?doid=3219819.3220102>.
- Ganin, Y. and Lempitsky, V. Unsupervised Domain Adaptation by Backpropagation. *International conference on machine learning*, pp. 1180–1189, 2015.
- Ghifary, M., Kleijn, W. B., Zhang, M., Balduzzi, D., and Li, W. Deep Reconstruction-Classification Networks for Unsupervised Domain Adaptation. *arXiv:1607.03516 [cs, stat]*, August 2016. URL <http://arxiv.org/abs/1607.03516>. arXiv: 1607.03516.
- Guo, H., Pasunuru, R., and Bansal, M. Multi-Source Domain Adaptation for Text Classification via DistanceNet-Bandits. *Proceedings of the AAAI Conference on Artificial Intelligence*, 34(05): 7830–7838, April 2020. ISSN 2374-3468, 2159-5399. doi: 10.1609/aaai.v34i05.6288. URL <https://aaai.org/ojs/index.php/AAAI/article/view/6288>.
- Gururangan, S., Marasović, A., Swayamdipta, S., Lo, K., Beltagy, I., Downey, D., and Smith, N. A. Don’t Stop Pretraining: Adapt Language Models to Domains and Tasks. In *Proceedings of the 58th Annual Meeting of the Association for Computational Linguistics*, pp. 8342–8360, Online, 2020. Association for Computational Linguistics. doi: 10.18653/v1/2020.acl-main.740. URL <https://www.aclweb.org/anthology/2020.acl-main.740>.
- Han, X. and Eisenstein, J. Unsupervised Domain Adaptation of Contextualized Embeddings for Sequence Labeling. In *Proceedings of the 2019 Conference on Empirical Methods in Natural Language Processing and the 9th International Joint Conference on Natural Language Processing (EMNLP-IJCNLP)*, pp. 4237–4247, Hong Kong, China, 2019. Association for Computational Linguistics. doi: 10.18653/v1/D19-1433. URL <https://www.aclweb.org/anthology/D19-1433>.
- Hoffman, J., Tzeng, E., Park, T., Zhu, J.-Y., Isola, P., Saenko, K., Efros, A. A., and Darrell, T. CyCADA: Cycle-Consistent Adversarial Domain Adaptation. *International conference on machine learning*, pp. 1989–1998, 2018.
- Hu, H., Tang, M., and Bai, C. DATSING: Data Augmented Time Series Forecasting with Adversarial Domain Adaptation. In *Proceedings of the 29th ACM International Conference on Information & Knowledge Management*, pp. 2061–2064, Virtual Event Ireland, October 2020. ACM. ISBN 978-1-4503-6859-9. doi: 10.1145/3340531.3412155. URL <https://dl.acm.org/doi/10.1145/3340531.3412155>.
- kaggle. Rossmann Store Sales, a. URL <https://kaggle.com/c/rossmann-store-sales>.
- kaggle. Web Traffic Time Series Forecasting, b. URL <https://kaggle.com/c/web-traffic-time-series-forecasting>.
- Li, S., Jin, X., Xuan, Y., Zhou, X., Chen, W., Wang, Y.-X., and Yan, X. Enhancing the Locality and Breaking the Memory Bottleneck of Transformer on Time Series Forecasting. *Advances in Neural Information Processing Systems*, pp. 5243–5253, 2019.
- Liberty, E., Karnin, Z., Xiang, B., Rouesnel, L., Coskun, B., Nallapati, R., Delgado, J., Sadoughi, A., Astashonok, Y., Das, P., Balioglu, C., Chakravarty, S., Jha, M., Gautier, P., Arpin, D., Januschowski, T., Flunkert, V., Wang, Y., Gasthaus, J., Stella, L., Rangapuram, S., Salinas, D., Schelter, S., and Smola, A. Elastic Machine Learning Algorithms in Amazon SageMaker. In *Proceedings of the 2020 ACM SIGMOD International Conference on Management of Data*, pp. 731–737, Portland OR USA, June 2020. ACM. ISBN 978-1-4503-6735-6. doi: 10.1145/3318464.3386126. URL <https://dl.acm.org/doi/10.1145/3318464.3386126>.

- Lim, B., Arik, S. O., Loeff, N., and Pfister, T. Temporal Fusion Transformers for Interpretable Multi-horizon Time Series Forecasting. *arXiv:1912.09363 [cs, stat]*, December 2019. URL <http://arxiv.org/abs/1912.09363>. arXiv: 1912.09363.
- Long, M., Cao, Y., Wang, J., and Jordan, M. I. Learning Transferable Features with Deep Adaptation Networks. *arXiv:1502.02791 [cs]*, May 2015. URL <http://arxiv.org/abs/1502.02791>. arXiv: 1502.02791.
- Motitian, S., Jones, Q., Iranmanesh, S. M., and Doretto, G. Few-Shot Adversarial Domain Adaptation. *Advances in Neural Information Processing Systems*, pp. 6670–6680, 2017. URL <http://arxiv.org/abs/1711.02536>. arXiv: 1711.02536.
- Oreshkin, B. N., Carpow, D., Chapados, N., and Bengio, Y. Meta-learning framework with applications to zero-shot time-series forecasting. *arXiv:2002.02887 [cs, stat]*, February 2020a. URL <http://arxiv.org/abs/2002.02887>. arXiv: 2002.02887.
- Oreshkin, B. N., Chapados, N., Carpow, D., and Bengio, Y. N-BEATS: Neural basis expansion analysis for interpretable time series forecasting. *International Conference on Learning Representations*, pp. 31, 2020b.
- Paszke, A., Gross, S., Massa, F., Lerer, A., Bradbury, J., Chanan, G., Killeen, T., Lin, Z., Gimelshein, N., Antiga, L., Desmaison, A., Kopf, A., Yang, E., DeVito, Z., Raison, M., Tejani, A., Chilamkurthy, S., Steiner, B., Fang, L., Bai, J., and Chintala, S. PyTorch: An Imperative Style, High-Performance Deep Learning Library. *Advances in neural information processing systems*, pp. 8026–8037, 2019.
- Ramponi, A. and Plank, B. Neural Unsupervised Domain Adaptation in NLP—A Survey. *arXiv:2006.00632 [cs]*, May 2020. URL <http://arxiv.org/abs/2006.00632>. arXiv: 2006.00632.
- Rangapuram, S. S., Seeger, M., Gasthaus, J., Stella, L., Wang, Y., and Januschowski, T. Deep State Space Models for Time Series Forecasting. pp. 13, 2018.
- Rennie, S., Marcheret, E., Mallinar, N., Nahamoo, D., and Goel, V. Unsupervised Adaptation of Question Answering Systems via Generative Self-training. In *Proceedings of the 2020 Conference on Empirical Methods in Natural Language Processing (EMNLP)*, pp. 1148–1157, Online, 2020. Association for Computational Linguistics. doi: 10.18653/v1/2020.emnlp-main.87. URL <https://www.aclweb.org/anthology/2020.emnlp-main.87>.
- Rietzler, A., Stabinger, S., Opitz, P., and Engl, S. Adapt or Get Left Behind: Domain Adaptation through BERT Language Model Finetuning for Aspect-Target Sentiment Classification. *Proceedings of The 12th Language Resources and Evaluation Conference*, pp. 4933–4941, 2020.
- Shi, G., Feng, C., Huang, L., Zhang, B., Ji, H., Liao, L., and Huang, H. Genre Separation Network with Adversarial Training for Cross-genre Relation Extraction. In *Proceedings of the 2018 Conference on Empirical Methods in Natural Language Processing*, pp. 1018–1023, Brussels, Belgium, 2018. Association for Computational Linguistics. doi: 10.18653/v1/D18-1125. URL <http://aclweb.org/anthology/D18-1125>.
- Tzeng, E., Hoffman, J., Saenko, K., and Darrell, T. Adversarial Discriminative Domain Adaptation. In *2017 IEEE Conference on Computer Vision and Pattern Recognition (CVPR)*, pp. 2962–2971, Honolulu, HI, July 2017. IEEE. ISBN 978-1-5386-0457-1. doi: 10.1109/CVPR.2017.316. URL <http://ieeexplore.ieee.org/document/8099799/>.
- Vaswani, A., Shazeer, N., Parmar, N., Uszkoreit, J., Jones, L., Gomez, A. N., Kaiser, L., and Polosukhin, I. Attention Is All You Need. *arXiv:1706.03762 [cs]*, December 2017. URL <http://arxiv.org/abs/1706.03762>. arXiv: 1706.03762.
- Wang, R., Maddix, D., Faloutsos, C., Wang, Y., and Yu, R. Bridging Physics-based and Data-driven modeling for Learning Dynamical Systems. *arXiv:2011.10616 [physics, q-bio]*, November 2020. URL <http://arxiv.org/abs/2011.10616>. arXiv: 2011.10616.
- Wang, Y., Smola, A., Maddix, D. C., Gasthaus, J., Foster, D., and Januschowski, T. Deep Factors for Forecasting. pp. 11, 2019.

- Wen, R., Torkkola, K., Narayanaswamy, B., and Madeka, D. A Multi-Horizon Quantile Recurrent Forecaster. *arXiv:1711.11053 [stat]*, November 2017. URL <http://arxiv.org/abs/1711.11053>. arXiv: 1711.11053.
- Wilson, G. and Cook, D. J. A Survey of Unsupervised Deep Domain Adaptation. *arXiv:1812.02849 [cs, stat]*, February 2020. URL <http://arxiv.org/abs/1812.02849>. arXiv: 1812.02849.
- Wright, D. and Augenstein, I. Transformer Based Multi-Source Domain Adaptation. In *Proceedings of the 2020 Conference on Empirical Methods in Natural Language Processing (EMNLP)*, pp. 7963–7974, Online, 2020. Association for Computational Linguistics. doi: 10.18653/v1/2020.emnlp-main.639. URL <https://www.aclweb.org/anthology/2020.emnlp-main.639>.
- Wu, S., Xiao, X., Ding, Q., Zhao, P., Wei, Y., and Huang, J. Adversarial Sparse Transformer for Time Series Forecasting. *Advances in Neural Information Processing Systems*, 33:11, 2020.
- Yu, H.-F., Rao, N., and Dhillon, I. S. Temporal Regularized Matrix Factorization for High-dimensional Time Series Prediction. *NIPS*, pp. 847–855, 2016.
- Zhang, Y., David, P., and Gong, B. Curriculum Domain Adaptation for Semantic Segmentation of Urban Scenes. In *2017 IEEE International Conference on Computer Vision (ICCV)*, pp. 2039–2049, Venice, October 2017. IEEE. ISBN 978-1-5386-1032-9. doi: 10.1109/ICCV.2017.223. URL <http://ieeexplore.ieee.org/document/8237485/>.
- Zhang, Y., Nie, S., Liu, W., Xu, X., Zhang, D., and Shen, H. T. Sequence-To-Sequence Domain Adaptation Network for Robust Text Image Recognition. In *2019 IEEE/CVF Conference on Computer Vision and Pattern Recognition (CVPR)*, pp. 2735–2744, Long Beach, CA, USA, June 2019. IEEE. ISBN 978-1-72813-293-8. doi: 10.1109/CVPR.2019.00285. URL <https://ieeexplore.ieee.org/document/8953495/>.
- Zhao, H., Zhang, S., Wu, G., Moura, J. M. F., Costeira, J. P., and Gordon, G. J. Adversarial Multiple Source Domain Adaptation. *Advances in neural information processing systems*, pp. 8559–8570, 2018.
- Zhou, H., Zhang, S., Peng, J., Zhang, S., Li, J., Xiong, H., and Zhang, W. Informer: Beyond Efficient Transformer for Long Sequence Time-Series Forecasting. In *Proceedings of the AAAI Conference on Artificial Intelligence*, 2021. URL <http://arxiv.org/abs/2012.07436>. arXiv: 2012.07436.

## Checklist

1. For all authors...
  - (a) Do the main claims made in the abstract and introduction accurately reflect the paper’s contributions and scope? [\[Yes\]](#)
  - (b) Did you describe the limitations of your work? [\[Yes\]](#) line 345-347
  - (c) Did you discuss any potential negative societal impacts of your work? [\[No\]](#) We don’t think there is likely to be any negative societal impacts of our work.
  - (d) Have you read the ethics review guidelines and ensured that your paper conforms to them? [\[Yes\]](#)
2. If you are including theoretical results...
  - (a) Did you state the full set of assumptions of all theoretical results? [\[N/A\]](#)
  - (b) Did you include complete proofs of all theoretical results? [\[N/A\]](#)
3. If you ran experiments...
  - (a) Did you include the code, data, and instructions needed to reproduce the main experimental results (either in the supplemental material or as a URL)? [\[Yes\]](#)
  - (b) Did you specify all the training details (e.g., data splits, hyperparameters, how they were chosen)? [\[Yes\]](#) In both main body and supplementary materials
  - (c) Did you report error bars (e.g., with respect to the random seed after running experiments multiple times)? [\[Yes\]](#) In supplementary materials

- (d) Did you include the total amount of compute and the type of resources used (e.g., type of GPUs, internal cluster, or cloud provider)? [Yes] line 248
- 4. If you are using existing assets (e.g., code, data, models) or curating/releasing new assets...
  - (a) If your work uses existing assets, did you cite the creators? [Yes]
  - (b) Did you mention the license of the assets? [Yes]
  - (c) Did you include any new assets either in the supplemental material or as a URL? [No]
  - (d) Did you discuss whether and how consent was obtained from people whose data you're using/curating? [No]
  - (e) Did you discuss whether the data you are using/curating contains personally identifiable information or offensive content? [No]
- 5. If you used crowdsourcing or conducted research with human subjects...
  - (a) Did you include the full text of instructions given to participants and screenshots, if applicable? [N/A]
  - (b) Did you describe any potential participant risks, with links to Institutional Review Board (IRB) approvals, if applicable? [N/A]
  - (c) Did you include the estimated hourly wage paid to participants and the total amount spent on participant compensation? [N/A]



## A Attention module

The attention module in our proposed Domain Adaptation Forecaster (DAF) model performs input reconstruction (interpolation) and future prediction (extrapolation) using the same set of queries, keys and values. It uses different choices of neighborhood positions  $\mathcal{N}(t)$  and position translations  $\mu(t)$ , as mentioned in section 4.1. The queries  $\mathbf{Q} = [\mathbf{q}_t]_{t=1}^T$  and keys  $\mathbf{K} = [\mathbf{k}_t]_{t=1}^T$  are dependent on the pattern embeddings produced by the convolutional layers in the encoder module, which encode a local window of raw time series. The specific settings of  $\mathcal{N}(t)$  and  $\mu(t)$  depend on the kernel sizes  $s$  of the involved convolutions. Figure 7(a) illustrates and example architecture with the number of convolutions  $M = 1$  and kernel sizes  $s = 3$ .

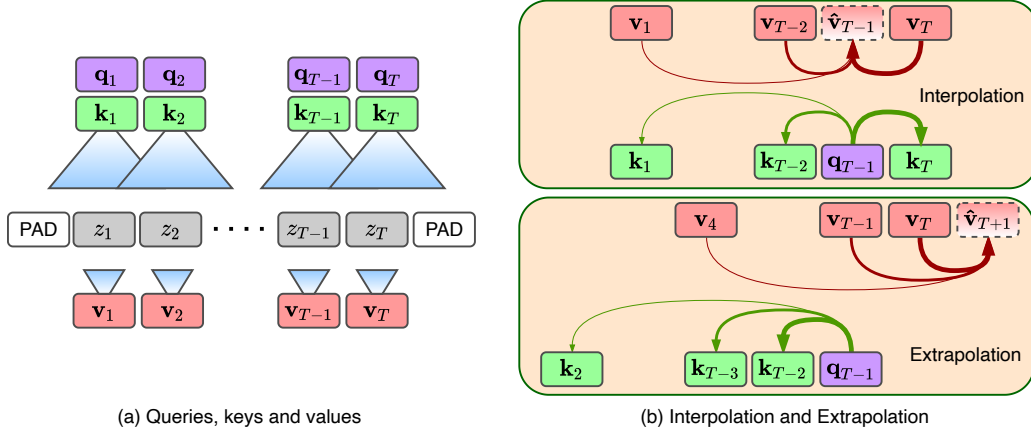


Figure 7: Interpolation and extrapolation within an attention module.

**Interpolation: Input Reconstruction** We reconstruct the input by interpolating  $\hat{z}_t$  using the observations at other time points. The upper panel of Figure 7(b) illustrates an example, where we would like to estimate  $\hat{z}_{T-1}$  using  $\{z_1, z_2, \dots, z_{T-2}, z_T\}$ . We take  $\mathbf{q}_{T-1}$  that depends on the local windows centered at the target step  $T - 1$  as shown in Figure 7(a) as the query, and compare it with the keys  $\{\mathbf{k}_1, \mathbf{k}_2, \dots, \mathbf{k}_{T-2}, \mathbf{k}_T\}$ . The attention scores  $\alpha(\mathbf{q}_{T-1}, \mathbf{k}_{t'})$  are computed by comparison using equation (6), and illustrated by the thickness of arrows in Figure 7(b). Similar to the query, the attended keys  $\mathbf{k}_{t'}$  depend on local windows centered at the respective step  $t'$ . Hence, the scores  $\alpha(\mathbf{q}_{T-1}, \mathbf{k}_{t'})$  depict the similarity of the value  $\hat{z}_{T-1}$  to the attended value  $z_{t'}$ , and we compute the output  $\mathbf{o}_{T-1}$  based on the combination of  $\mathbf{v}_{t'}$  weighted by  $\alpha(\mathbf{q}_{T-1}, \mathbf{k}_{t'})$  according to equation (5).

To generalize the example at time  $T - 1$  in Figure 7(b), we formally set

$$\begin{aligned}\mathcal{N}(t) &= \{1, 2, \dots, T\} \setminus \{t\}, \\ \mu(t') &= t',\end{aligned}$$

in equation (??). Although the ground truth  $z_t$  is encoded in the query, and the nearby keys within the local window are centered at time step  $t$ , it is not incorporated in  $\mathbf{o}_t$ , which instead depends on values at  $\mathcal{N}(t)$ .

**Extrapolation: Future Predictions** Since DAF is an autoregressive forecaster, it generates forecasts one step ahead. At each step, we forecast the next value by extrapolating from the given historical values. The lower panel of Figure 7(b) illustrates an example, where we would like to estimate the  $(T + 1)$ -th value given the past  $T$  observations and expected. The prediction  $\hat{z}_{T+1}$  follows the last local window  $\{z_{T-s+1}, z_{T-s+2}, \dots, z_T\}$  on which the query  $\mathbf{q}_{T-\bar{s}}$  is dependent, where  $\bar{s} = \lceil \frac{s-1}{2} \rceil$ , and  $\lceil \cdot \rceil$  denotes the ceiling operator. We take  $\mathbf{q}_{T-\bar{s}}$  as the query for  $T + 1$ , i.e. we set  $\mathbf{q}_{T+1} = \mathbf{q}_{T-\bar{s}}$ , and attend to the previous keys that do not encode padding zeros, i.e. we set:

$$\mathcal{N}(T + 1) = \{s, \dots, T - \bar{s} - 1\}.$$

In this case, the attention score  $\alpha(\mathbf{q}_{T+1}, \mathbf{k}_{t'})$  from equation (5) depicts the similarity of the unknown  $\hat{z}_{T+1}$ , and the value  $z_{t'+\bar{s}+1}$  following the local window  $\{z_{t'-\bar{s}}, \dots, z_{t'}, \dots, z_{t'+\bar{s}}\}$  corresponding to the attended key  $\mathbf{k}_{t'}$ . Hence, we set

$$\mu(t') = t' + \bar{s} + 1,$$

in equation (??) to estimate  $\mathbf{o}_{T+1}$ .

Figure 7 illustrates an example of future forecasts, where  $s = 3$  and  $M = 1$  in encoder module, as shown in Figure 7(a). Meanwhile, the lower panel of Figure 7(b) describes how attention is performed to estimate  $\mathbf{v}_{T+1}$ , which will lead to  $\mathbf{o}_{T+1}$  according to equation (7).

## B Dataset Details

### B.1 Synthetic Datasets

The synthetic datasets consist of sinusoidal signals with uniformly sampled parameters as follows:

$$\begin{aligned} z_{i,t} &= A_i \sin(2\pi\omega_i t + \phi_i) + c_i + \epsilon_{i,t}, \quad t \in [0, T + \tau], \\ A_i &\sim \text{Unif}(A_{\min}, A_{\max}), \quad c_i \sim \text{Unif}(c_{\min}, c_{\max}), \\ \omega_i &\sim \text{Unif}(\omega_{\min}, \omega_{\max}), \quad \phi_i \sim \text{Unif}(-2\pi, 2\pi), \end{aligned}$$

where  $A_{\min}, A_{\max} \in \mathbb{R}^+$  denote the amplitudes,  $c_{\min}, c_{\max} \in \mathbb{R}$  denote the levels, and  $\omega_{\min}, \omega_{\max} \in [\frac{1}{T}, \frac{20}{T}]$  denote the frequencies. In addition,  $\epsilon_{i,t} \sim \mathcal{N}(0, 0.2)$  is a white noise term. In our experiments, we fix  $T = 144, \tau = 18, A_{\min} = 0.5, A_{\max} = 5.0, c_{\min} = -3.0, c_{\max} = 3.0$ .

### B.2 Real-World Datasets

Table 4 summarizes the four benchmark real-world datasets that we use to evaluate our DAF model.

Dataset	Freq	Value	# Time Series	Average Length	Comment
<i>elec</i>	hourly	$\mathbb{R}^+$	370	3304	Household electricity consumption
<i>traf</i>	hourly	$[0, 1]$	963	360	Occupancy rate of SF Bay Area highways
<i>sales</i>	daily	$\mathbb{N}^+$	500	1106	Daily sales of Rossmann grocery stores
<i>wiki</i>	daily	$\mathbb{N}^+$	9906	70	Visit counts of various Wikipedia pages

Table 4: Benchmark dataset descriptions.

For evaluation, we follow Flunkert et al. (2017), and we take moving windows of length  $T + \tau$  starting at different points from the original time series in the datasets. For an original time series  $[z_{i,t}]_{t=1}^L$  of length  $L$ , we obtain a set of moving windows:

$$\{[z_{i,t}]_{t=n}^{n+T+\tau-1} \mid n = 1, 2, \dots, L - T - \tau + 1\}.$$

This procedure results in a set of fixed-length trajectory samples. Each sample is further split into historical observations  $X$  and forecasting targets  $Y$ , where the lengths of  $X$  and  $Y$  are  $T$  and  $\tau$ , respectively. We randomly select samples from the population by uniform sampling for training, validation and test sets.

## C Implementation Details

### C.1 Baselines

In this subsection, we provide an overview of the following baseline models:

- Conventional single-domain forecasters trained only on the target domain:
  - DeepAR is an auto-regressive RNN-based model with LSTM units. Unlike DAF and the rest of our baselines which we implement in Pytorch, we directly call DeepAR from Amazon Sagemaker.

- N-BEATS is an MLP-based forecaster. Similar to DAF, it aims to forecast the future as well as to reconstruct the given history. N-BEATS only consumes univariate time series  $z_{i,t}$ , and does not accept covariates  $\xi_{i,t}$  as input. In the original paper [Oreshkin et al. \(2020b\)](#), it employs various objectives and ensembles to improve the results. In our implementation, we use the ND metric as the training objective, and do not use any ensembling techniques for a fair comparison.
- ConvTrans is an attention-based forecaster that builds attention blocks on convolutional activations as DAF does. Unlike DAF, it does not reconstruct the input, and only fits the future. From a probabilistic perspective, it models the conditional distribution  $P(Y|X)$  instead of the joint distribution  $P(X, Y)$  as DAF does, where  $X$  and  $Y$  are history and future, respective. In addition, it directly uses the outputs of the convolution as queries and keys in the attention module.
- AttF is the single-domain version of DAF. It is equivalent to the branch of the sequence generator for the target domain in DAF. It has access to the attention module, but does not share it with another branch.
- Cross-domain forecasters trained on both source and target domain:
  - MetaF has the same architecture as N-BEATS. It trains a model on the source dataset, and applies it to the target dataset in a zero-shot setting, i.e. without any fine-tuning. Both MetaF and N-BEATS rely on given Fourier bases to fit seasonal patterns. For instance, bases of period 24 and 168 are included for hourly datasets, whereas bases of period 7 are included for daily datasets. The daily and weekly patterns are expected to be captured in all settings.
  - PTF has the same architecture as AttF for the target data. Unlike AttF, PTF fits both source and target data. It is first pretrained on the source dataset, and then finetuned on the target dataset.
  - RDA has the same overall structure as DAF, but replaces the attention module in DAF with a LSTM module. The encoder module produces a single output, which is then consumed by the LSTM. The domain discriminator aims to distinguish the output of encoder.
  - NA-DAF removes the domain discriminator from DAF for the ablation studies. It is trained only by minimizing the estimation error  $\mathcal{L}_{seq}$ , and ignores the domain classification error  $\mathcal{L}_{dom}$  term in equation (2) as the adversarial component is eliminated.

	$h$	$l_{MLP}$	$s$	$\gamma$	$\lambda$
cold-start	64	1	(3,5)	1e-3	1.0
few-shot					
<i>elec</i>	128	1	13	1e-3	1.0
<i>traf</i>	64	1	(3,17)	1e-2	10.0
<i>wiki</i>	64	2	(3,5)	1e-3	1.0
<i>sales</i>	128	2	(3,5)	1e-3	1.0

Table 5: Hyperparameters of DAF models in various synthetic and real-world experiments.

## C.2 Hyperparameters

The hyperparameters of DAF and baseline models are selected by grid-search over the validation set. In particular, we are interested in the following hyperparameters:

- the hidden dimension  $h \in \{32, 64, 128, 256\}$  of all models,
- the number of MLP layers  $l_{MLP} \in \{4\}$  for N-BEATS <sup>1</sup>,  $l_{MLP} \in \{1, 2, 3\}$  for DAF and its variants,
- the number of RNN layers  $l_{RNN} \in \{1, 3\}$  in DeepAR and RDA,
- the kernel sizes of convolutions  $s \in \{3, 13, (3, 5), (3, 17)\}$  in ConvTrans, DAF and its variants, <sup>2</sup>

<sup>1</sup>We set the other hyperparameters for N-BEATS as suggested in the original paper [Oreshkin et al. \(2020b\)](#).

<sup>2</sup>A single integer means a single convolution layer in the encoder module, while a tuple stands for multiple convolutions.

- the learning rate  $\gamma \in \{0.001, 0.01, 0.1\}$  for all models,
- the trade-off coefficient  $\lambda \in \{1, 10, 100\}$  in equation (2) for RDA and DAF.

The models are trained for at most  $100K$  iterations, which we empirically found to be more than sufficient for all models to converge. We use early stopping with respect to the ND metric on the validation set.

Table 5 summarizes the specific configurations of the hyper-parameters for our proposed DAF model in all experiments.

## D Detailed Experiment Results

### D.1 Quantitative Results

Tables 6-7 display the full experimental results of the mean plus or minus one standard deviation over 5 runs with different random initializations to supplement the mean ND results in Tables 1-2.

Task	$N$	$T$	$\tau$	DAR	VT	CT	MetaF	PTF	RDA	DAF
Cold Start	5000	36	18	0.053 $\pm$ 0.003	0.040 $\pm$ 0.001	0.042 $\pm$ 0.001	0.045 $\pm$ 0.005	0.039 $\pm$ 0.006	<b>0.035<math>\pm</math>0.002</b>	<b>0.035<math>\pm</math>0.003</b>
		45		0.037 $\pm$ 0.002	0.039 $\pm$ 0.001	0.041 $\pm$ 0.004	0.043 $\pm$ 0.006	0.037 $\pm$ 0.005	0.034 $\pm$ 0.001	<b>0.030<math>\pm</math>0.003</b>
		54		<b>0.031<math>\pm</math>0.002</b>	0.039 $\pm$ 0.001	0.038 $\pm$ 0.005	0.042 $\pm$ 0.002	0.034 $\pm$ 0.008	0.034 $\pm$ 0.001	<b>0.029<math>\pm</math>0.003</b>
Few Shot	20	144	18	0.062 $\pm$ 0.003	0.089 $\pm$ 0.001	0.095 $\pm$ 0.003	0.071 $\pm$ 0.004	0.086 $\pm$ 0.004	<b>0.059<math>\pm</math>0.003</b>	<b>0.057<math>\pm</math>0.004</b>
	50			0.059 $\pm$ 0.004	0.085 $\pm$ 0.001	0.074 $\pm$ 0.005	0.061 $\pm$ 0.003	0.086 $\pm$ 0.003	<b>0.054<math>\pm</math>0.003</b>	<b>0.055<math>\pm</math>0.001</b>
	100			0.059 $\pm$ 0.003	0.079 $\pm$ 0.002	0.071 $\pm$ 0.002	0.053 $\pm$ 0.003	0.081 $\pm$ 0.005	0.053 $\pm$ 0.007	<b>0.051<math>\pm</math>0.001</b>

Table 6: Performance comparison of DAF on synthetic datasets with varying historical lengths  $T$  (cold-start), and varying number of time series  $N$  (few-shot) and prediction length  $\tau$  in terms of the mean  $\pm$  the standard deviation ND metric. The winners and the competitive followers (the gap is smaller than its standard deviation over 5 runs) are bolded for reference.

$D_T$	$D_S$	$F$	$T$	$\tau$	DAR	VT	CT	MetaF	PTF	RDA	DAF
traf	elec	H	168	24	0.205 $\pm$ 0.015	0.187 $\pm$ 0.003	0.183 $\pm$ 0.013	0.190 $\pm$ 0.005	0.184 $\pm$ 0.003	0.174 $\pm$ 0.005	<b>0.169<math>\pm</math>0.002</b>
	wiki							0.188 $\pm$ 0.002	0.185 $\pm$ 0.004	0.181 $\pm$ 0.003	<b>0.176<math>\pm</math>0.004</b>
elec	traf	H	168	24	0.141 $\pm$ 0.023	0.144 $\pm$ 0.004	0.131 $\pm$ 0.005	0.151 $\pm$ 0.004	0.144 $\pm$ 0.005	0.154 $\pm$ 0.002	<b>0.125<math>\pm</math>0.008</b>
	sales							0.144 $\pm$ 0.004	0.138 $\pm$ 0.007	0.142 $\pm$ 0.003	<b>0.123<math>\pm</math>0.005</b>
wiki	sales	D	28	7	0.055 $\pm$ 0.010	0.061 $\pm$ 0.008	0.051 $\pm$ 0.006	0.061 $\pm$ 0.003	<b>0.047<math>\pm</math>0.002</b>	<b>0.049<math>\pm</math>0.003</b>	<b>0.049<math>\pm</math>0.003</b>
	traf							0.059 $\pm$ 0.005	<b>0.044<math>\pm</math>0.003</b>	<b>0.045<math>\pm</math>0.003</b>	<b>0.042<math>\pm</math>0.004</b>
sales	wiki	D	28	7	0.305 $\pm$ 0.005	0.293 $\pm$ 0.005	0.324 $\pm$ 0.013	0.311 $\pm$ 0.001	0.292 $\pm$ 0.007	0.287 $\pm$ 0.002	<b>0.280<math>\pm</math>0.007</b>
	elec							0.329 $\pm$ 0.002	0.287 $\pm$ 0.004	0.285 $\pm$ 0.001	<b>0.277<math>\pm</math>0.005</b>

Table 7: Performance comparison of DAF on real-world benchmark datasets with the historical time series length  $T$ , prediction length  $\tau$ , in the target domain determined by the target dataset frequencies  $F$  in terms of the mean  $\pm$  standard deviation ND metric. The winners and the competitive followers (the gap is smaller than its standard deviation over 5 runs) are bolded for reference.

### D.2 Qualitative Results

We also provide visualizations of forecasts for both synthetic and real-world experiments. Figure 8 provides more samples for the few-shot experiment where  $N = 20$  as a complement to Figure 4. We see that DAF is able to approximately capture the sinusoidal signals even if the input is contaminated by white noise in most cases, while AttF fails in many cases. Figure 9 illustrates the performance gap between DAF and AttF in the experiment with source data *elec* and target data *traf* as an example in real scenarios. While AttF generally captures daily patterns, DAF performs significantly better.

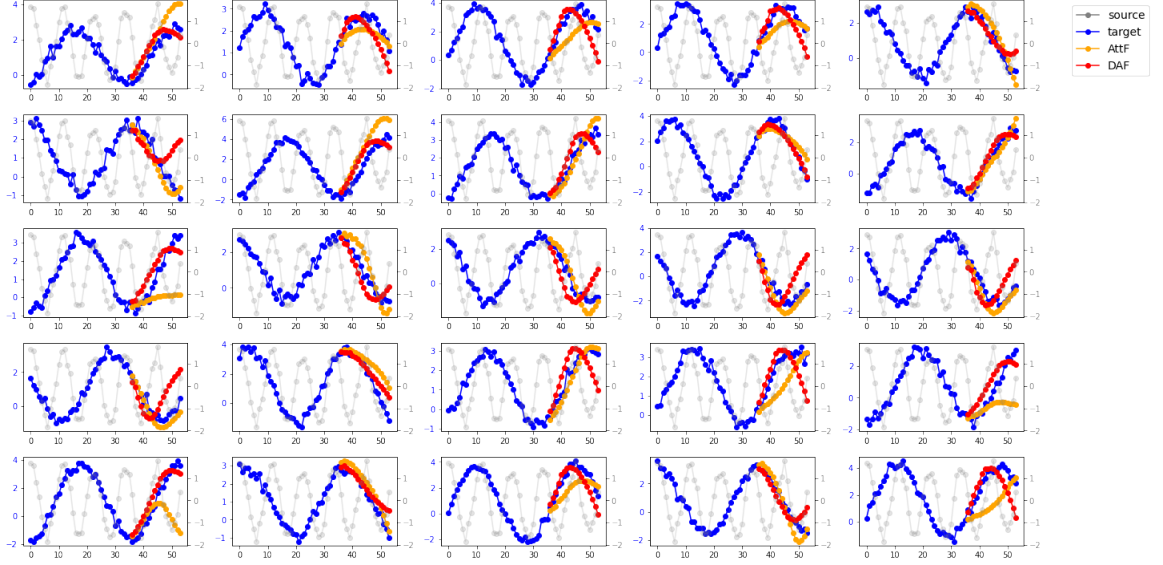


Figure 8: Test samples in the synthetic few-shot experiment where  $N = 20$ . The y-axis corresponding to the source is shown in grey, and that for the target in blue.

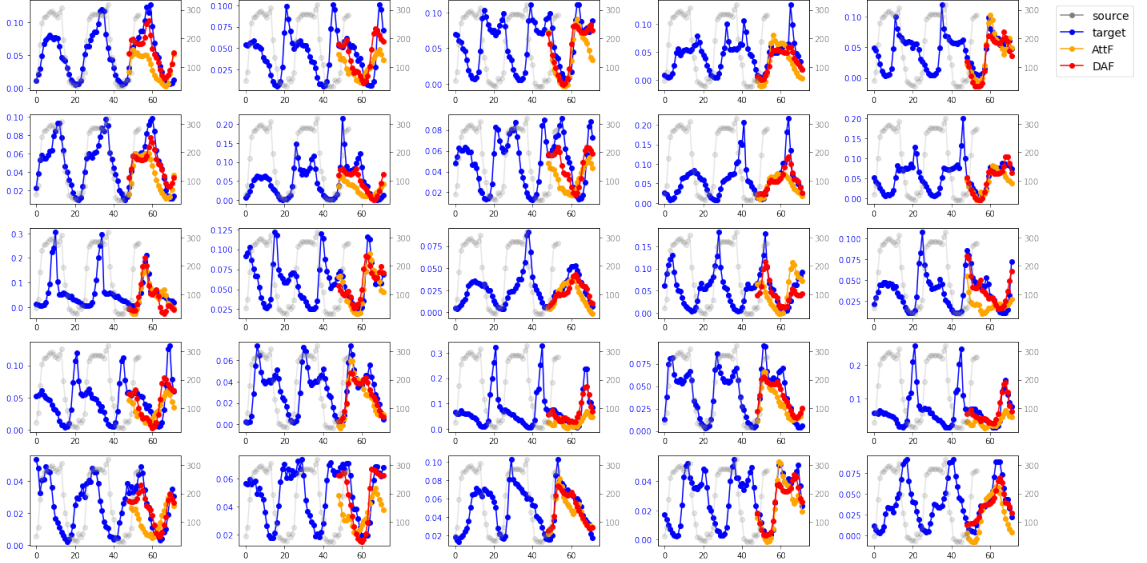


Figure 9: Test samples with source data *elec* and target data *traf* experiment. The y-axis corresponding to the source is shown in grey, and that for the target in blue.